

Interference-Robust Non-Coherent Over-the-Air Computation for Decentralized Optimization

Nicolò Michelusi, *Senior Member, IEEE*

Abstract—Non-coherent over-the-air (NCOTA) computation enables low-latency and bandwidth-efficient decentralized optimization by exploiting the average energy superposition property of wireless channels. It has recently been proposed as a powerful tool for executing consensus-based optimization algorithms in fully decentralized systems. A key advantage of NCOTA is that it enables unbiased consensus estimation without channel state information at either transmitters or receivers, requires no transmission scheduling, and scales efficiently to dense network deployments. However, NCOTA is inherently susceptible to external interference, which can bias the consensus estimate and deteriorate the convergence of the underlying decentralized optimization algorithm. In this paper, we propose a novel interference-robust (IR)-NCOTA scheme. The core idea is to apply a coordinated random rotation of the frame of reference across all nodes, and transmit a pseudo-random pilot signal, allowing to transform external interference into a circularly symmetric distribution with zero mean relative to the rotated frame. This ensures that the consensus estimates remain unbiased, preserving the convergence guarantees of the underlying optimization algorithm. Through numerical results on a classification task, it is demonstrated that IR-NCOTA exhibits superior performance over the baseline NCOTA algorithm in the presence of external interference.

Index Terms—Decentralized Learning, Decentralized gradient descent, non-coherent over-the-air computation

I. INTRODUCTION

Decentralized optimization and learning arise in various domains such as remote sensing, distributed inference [1], estimation [2], multi-agent coordination [3], and machine learning (ML) [4]. In traditional learning frameworks, data is aggregated in a centralized location where computationally intensive optimization algorithms are executed. Yet, in emerging verticals where infrastructure is absent, unreliable, or has been disrupted, such as post-disaster environments [5], search and rescue operations, or remote rural regions [6], centralized aggregation may be impractical. These limitations require a shift toward decentralized alternatives, in which agents such as uncrewed aerial vehicles (UAVs) perform sensing, inference, and learning locally, while relying only on peer-to-peer communications [7]. Within this context, this paper aims to solve the optimization problem

$$\mathbf{w}^* = \arg \min_{\mathbf{w} \in \mathbb{R}^d} F(\mathbf{w}) \triangleq \frac{1}{N} \sum_{i=1}^N f_i(\mathbf{w}) \quad (1)$$

among N wirelessly-connected nodes, where $f_i(\mathbf{w})$ is the local function of node i , known to i alone, and \mathbf{w} is a d -dimensional parameter vector. For instance, f_i may represent the empirical loss based on the local dataset of node i , and $F(\mathbf{w})$ is the empirical loss over the global dataset.

N. Michelusi is with the School of Electrical, Computer and Energy Engineering, Arizona State University. email: nicolo.michelusi@asu.edu. This research has been funded in part by NSF under grant CNS-2129015.

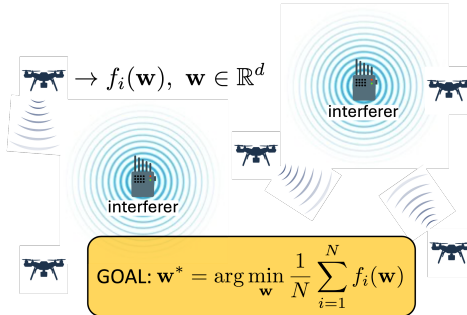


Fig. 1: Example of a swarm of UAVs collaboratively solving a decentralized optimization problem, with two interferers generating unwanted interference.

A renowned algorithm to solve (1) in decentralized settings is *Decentralized Gradient Descent* (DGD) [8], [9]. In DGD, each node i iteratively updates its local parameter vector \mathbf{w}_i through consensus and local gradient descent. However, implementing DGD over wireless channels poses significant challenges due to noise, fading, interference, and the need for multi-access coordination [10]–[17].

In a wireless implementation of DGD [18], [19], each node updates its local parameter vector at iteration k as

$$\mathbf{w}_{i,k+1} = \mathbf{w}_{i,k} + \gamma_k \hat{\mathbf{d}}_{i,k} - \eta_k \nabla f_i(\mathbf{w}_{i,k}), \quad (\text{DGD})$$

where $-\eta_k \nabla f_i(\mathbf{w}_{i,k})$ represents a local gradient descent step controlled by the learning stepsize η_k , and $\hat{\mathbf{d}}_{i,k}$ is an estimate of the *disagreement signal*, defined as

$$\mathbf{d}_{i,k} = - \sum_{j=1}^N \ell_{ij} \mathbf{w}_{j,k} = - \sum_{j \neq i} \ell_{ij} (\mathbf{w}_{j,k} - \mathbf{w}_{i,k}), \quad (2)$$

where $\{\ell_{ij}\}$ denote symmetric Laplacian weights, satisfying $\ell_{ij} = \ell_{ji} \leq 0$ for all $i \neq j$ and $\ell_{ii} = - \sum_{j \neq i} \ell_{ij}$. The parameter $\gamma_k > 0$ is a consensus step size that mitigates the effect of errors in the disagreement signal estimation caused by imperfect wireless communications (e.g., noise, fading, or interference). Since $\sum_j \ell_{ij} = 0$, if all local parameter vectors $\mathbf{w}_{j,k}$ take a common value $\bar{\mathbf{w}}$, then $\mathbf{d}_{i,k} = \mathbf{0}$. Thus, $\mathbf{d}_{i,k}$ quantifies the degree of disagreement of $\{\mathbf{w}_{i,k}\}$ across the network.

An estimate of $\mathbf{d}_{i,k}$ is discussed in Secs. II and III. In essence, DGD combines a correction step based on this estimate ($\hat{\mathbf{d}}_{i,k}$), which promotes agreement and reduces model discrepancies, with a local gradient descent step that drives convergence toward optimality. Iterating these steps steers the system toward consensus and global optimality.

In our prior work [18], [19], we demonstrated that, for strongly convex f_i , the noisy DGD algorithm converges to the global optimum \mathbf{w}^* with an error $\frac{1}{N} \sum_i \mathbb{E}[\|\mathbf{w}_{i,k} - \mathbf{w}^*\|^2] =$

$\mathcal{O}(1/\sqrt{k})$, for a suitable choice of η_k, γ_k . However, this convergence result relies on *unbiasedness* of the disagreement signal estimate, i.e., $\mathbb{E}[\hat{\mathbf{d}}_{i,k} | \mathbf{w}_{j,k}, \forall j] = \mathbf{d}_{i,k}$, as it ensures that fluctuations of the estimate $\hat{\mathbf{d}}_{i,k}$ around its expected value $\mathbf{d}_{i,k}$ are averaged out over DGD iterations. Conversely, if this unbiasedness condition is not satisfied, a distortion is introduced that accumulates over time, preventing convergence.

Recently, non-coherent over-the-air computation (NCOTA) has been proposed in [19] to estimate the disagreement signal over wireless channels affected by noise and fading. In this scheme, each local parameter vector $\mathbf{w}_{i,k}$ controls the energy of the transmitted signal. Nodes transmit in a randomized and simultaneous fashion, and their signals naturally superimpose over the wireless medium, producing an *unbiased estimate* of the disagreement signal by exploiting the *average energy superposition* property of wireless channels. This enables unbiased estimation of $\mathbf{d}_{i,k}$ without requiring topology information, channel state information at the transmitters or receivers, or transmission scheduling, at the cost of additional noise in the disagreement signal estimation due to channel impairments such as noise, fading, and energy fluctuations. Numerical results in [19] demonstrate that NCOTA outperforms implementations based on orthogonal transmissions [20] and conventional over-the-air computation [12], [21], particularly as the number of agents increases.

However, the unbiasedness of NCOTA no longer holds under external interference, as interference energy accumulates at the receivers, introducing an uncontrolled drift in the DGD updates that undermines convergence. In this paper, we propose a novel *Interference-Robust* (IR) NCOTA scheme that preserves the effectiveness of NCOTA even under external interference. The key idea is to leverage coordinated randomness across the network to *scramble* the interference signals. Specifically, we introduce two key mechanisms: (1) a coordinated random rotation of the frame of reference, which maps energy values to different reference orientations so that, when averaged over the pseudo-random rotations, the additive interference contribution appears zero-mean; and (2) a pseudo-random pilot sequence, used to estimate the aggregate channel gains (self Laplacian weights ℓ_{ii}) while ensuring that the interference contribution remains zero-mean. We show that IR-NCOTA produces an unbiased estimate of the disagreement signal, enabling direct application of the convergence results established in [19].

The remainder of this paper is structured as follows. Sec. II provides a background of NCOTA. Sec. III presents the proposed algorithm, and demonstrates its unbiasedness properties. Sec. IV provides numerical results. Finally, Sec. V provides concluding remarks. We refer to our prior work [19] for an in-depth discussion of NCOTA and its convergence properties. Notation: We use boldface letters for vectors (e.g., $\mathbf{a} \in \mathbb{C}^d$) and non-boldface letters for scalars (e.g., $a \in \mathbb{C}$). For a (column) vector \mathbf{a} , we define: its m th element as $[\mathbf{a}]_m$; its conjugate transpose as \mathbf{a}^H ; its transpose as \mathbf{a}^\top ; its Euclidean norm as $\|\mathbf{a}\| = \sqrt{\mathbf{a}^H \mathbf{a}}$; and its ℓ_1 norm as $\|\mathbf{a}\|_1 = \sum_m |[\mathbf{a}]_m|$. For a scalar $a \in \mathbb{C}$, we denote its complex conjugate as a^* . We use $\mathbf{1}$ and $\mathbf{0}$ to denote the all-ones and all-zeros vectors, respectively, \mathbf{e}_m for the m th standard basis vector, and \mathbf{I} to denote the

identity matrix (with dimension clear from context). Finally, $\mathcal{CN}(\mathbf{b}, \Sigma)$ denotes a circularly symmetric complex Gaussian random vector with mean \mathbf{b} and covariance matrix Σ .

II. BACKGROUND OF NCOTA [19]

We assume that $\|\mathbf{w}^*\| \leq r$ for some known r , hence the optimization is restricted to the d -dimensional sphere $\mathcal{W} \equiv \{\mathbf{w} \in \mathbb{R}^d : \|\mathbf{w}\| \leq r\}$. This guarantees that signals remain bounded during communication, thereby ensuring practical energy constraints. For notational convenience, we omit the dependence on the iteration index k . NCOTA estimates the disagreement signal over wireless channels as follows [19].

Energy-based encoding: First, the local parameter vector $\mathbf{w}_i \in \mathcal{W}$ is expressed as the convex combination

$$\mathbf{w}_i = \sum_{m=1}^M [\mathbf{p}_i]_m \mathbf{z}_m, \quad (3)$$

where $\{\mathbf{z}_1, \dots, \mathbf{z}_M\}$ is a set of $M \triangleq 2d+1$ codewords defined as $\mathbf{z}_M = \mathbf{0}$ and, for $m = 1, \dots, d$,

$$\mathbf{z}_m = \sqrt{d}r \mathbf{e}_m, \quad \mathbf{z}_{d+m} = -\sqrt{d}r \mathbf{e}_m. \quad (4)$$

whereas \mathbf{p}_i is a set of non-negative coefficients defined as $[\mathbf{p}_i]_M = 1 - \frac{1}{\sqrt{dr}} \|\mathbf{w}_i\|_1$, and, for $m = 1, \dots, d$,

$$[\mathbf{p}_i]_m = \frac{1}{\sqrt{dr}} ([\mathbf{w}_i]_m)^+, \quad [\mathbf{p}_i]_{d+m} = \frac{1}{\sqrt{dr}} (-[\mathbf{w}_i]_m)^+, \quad (5)$$

where $(\cdot)^+ = \max\{\cdot, 0\}$. With this definition, and using the fact that $a = (a)^+ - (-a)^+$, it is straightforward to verify that (3) holds. Furthermore, since $\|\mathbf{w}_i\|_1 \leq \sqrt{d} \|\mathbf{w}_i\| \leq \sqrt{dr}$ (by the Cauchy-Schwarz inequality) and $(\cdot)^+ \geq 0$, it follows that $\mathbf{p}_i \geq 0$ and $\mathbf{1}^\top \mathbf{p}_i = 1$. We compactly denote the encoding scheme applied by each node through (5) as

$$\mathbf{p}_i \triangleq \mathcal{P}(\mathbf{w}_i). \quad (6)$$

Since $\mathbf{p}_i \geq 0$, this representation is suitable for fully decentralized energy-based transmission, unlike the signal \mathbf{w}_i , which may contain negative elements. Each transmitter thus generates its transmit signal as

$$\mathbf{x}_i = \sqrt{EM} \sqrt{\mathbf{p}_i}, \quad (7)$$

where $\sqrt{\cdot}$ is element-wise, so that \mathbf{p}_i controls sample energy. Since $\mathbf{1}^\top \mathbf{p}_i = 1$, the energy per sample is $\|\mathbf{x}_i\|^2/M = E$.

Randomized transmission: To satisfy half-duplex constraints, we adopt a probabilistic transmission strategy: with probability p_{tx} , node i operates as a transmitter (indicated by $\chi_i = 0$); otherwise, it operates as a receiver (i.e., $\chi_i = 1$). These transmission decisions are i.i.d. across nodes and iterations, enabling a fully decentralized implementation.

Received signal: Assuming Rayleigh flat-fading channels $h_{ij} \sim \mathcal{CN}(0, \Lambda_{ij})$ between transmitter j and receiver i ,¹ with average channel gain Λ_{ij} , independent across node pairs i, j , the received signal at receiver i is

$$\mathbf{y}_i = \sum_{j: \chi_j=0} h_{ij} \mathbf{x}_j + \mathbf{n}_i, \quad (8)$$

¹Our paper [19] discusses extensions to a broad class of frequency-selective channels.

where $\mathbf{n}_i \sim \mathcal{CN}(\mathbf{0}, N_0 \mathbf{I})$ denotes Gaussian noise with power spectral density N_0 . We will include interference in Sec. III.

Disagreement signal estimation: Upon receiving the signal \mathbf{y}_i , each node computes the received sample energy as

$$[\mathbf{r}_i]_m = \chi_i \frac{|[\mathbf{y}_i]_m|^2 - N_0}{(1 - p_{tx})p_{tx}E \cdot M}, \quad \forall m = 1, \dots, M, \quad (9)$$

and estimates the disagreement signal as

$$\hat{\mathbf{d}}_i = \sum_{m=1}^M [\mathbf{r}_i]_m (\mathbf{z}_m - \mathbf{w}_i). \quad (10)$$

Note that $\mathbf{r}_i = \mathbf{0}$ and $\hat{\mathbf{d}}_i = \mathbf{0}$ for nodes operating as transmitters in the current iteration.

Taking the expectation of \mathbf{r}_i with respect to Gaussian noise \mathbf{n}_i , Rayleigh fading channels h_{ij} , the randomized transmit/receive decisions $\chi_j \in \{0, 1\}$; and using the energy-based signal encoding (7), it can be shown that

$$\mathbb{E}[\mathbf{r}_i | \mathbf{w}_j, \forall j] = \sum_{j \neq i} \Lambda_{ij} \mathbf{p}_j.$$

Then, using (10), the convex combination structure (3), and the fact that $\sum_{m=1}^M [\mathbf{p}_j]_m = 1$, we obtain

$$\begin{aligned} \mathbb{E}[\hat{\mathbf{d}}_i | \mathbf{w}_j, \forall j] &= \sum_{j \neq i} \Lambda_{ij} \sum_{m=1}^M [\mathbf{p}_j]_m (\mathbf{z}_m - \mathbf{w}_i) \\ &= \sum_{j \neq i} \Lambda_{ij} (\mathbf{w}_j - \mathbf{w}_i) \triangleq \mathbf{d}_i. \end{aligned} \quad (11)$$

Comparing this result with (2), we conclude that $\hat{\mathbf{d}}_i$ is an unbiased estimate of the disagreement signal, with Laplacian weights $\ell_{ij} = -\Lambda_{ij}$ given by the average channel gains.

This unbiasedness property is critical to achieve the convergence properties of the DGD algorithm, established in [19]. In the next section, we consider a more general signal model that includes external interference. We will show that, under external interference, the estimate given in (10) becomes biased, introducing a drift in the DGD updates that accumulates over time and leads to a loss of convergence. We will then propose a novel interference-robust NCOTA scheme that recovers the unbiasedness condition.

III. SIGNAL MODEL AND IR-NCOTA

We consider a more general model than (8), including external interference, as illustrated in Fig. 1. Specifically, we model \mathbf{n}_i as a combined noise-plus-interference term. We impose no specific distributional assumptions on \mathbf{n}_i , other than a bounded second-order moment and the requirement that it be uncorrelated with the Rayleigh channel coefficients, i.e., $\mathbb{E}[h_{ij}^* \mathbf{n}_i] = \mathbf{0}$. The term \mathbf{n}_i may have a non-zero mean, exhibit correlation or non-stationarity, be non-Gaussian, and may even depend on the local optimization signals \mathbf{w}_j , for example in the presence of adversarial devices. This model captures a wide range of interference sources, including jamming and adversarial transmitters [22].

Under such more general model, NCOTA fails to compute an *unbiased* estimate of the disagreement signal, as shown in the following example.

Example 1. Consider the noise-plus-interference model

$$\mathbf{r}_i = g_i \sqrt{E \cdot M} [1, 0, 0, \dots, 0]^\top + \mathcal{CN}(\mathbf{0}, N_0 \mathbf{I}),$$

where $g_i \sim \mathcal{CN}(0, \Gamma_i)$ represents the Rayleigh fading channel between the interferer and node i , generating interference only on the first received sample. Then, under NCOTA, the expectation of \mathbf{r}_i yields

$$\mathbb{E}[\mathbf{r}_i | \mathbf{w}_j, \forall j] = \sum_{j \neq i} \Lambda_{ij} \mathbf{p}_j + \frac{\Gamma_i}{p_{tx}} [1, 0, 0, \dots, 0]^\top,$$

and consequently, after applying (10) and similarly to (11),

$$\mathbb{E}[\hat{\mathbf{d}}_i | \mathbf{w}_j, \forall j] = \sum_{j \neq i} \Lambda_{ij} (\mathbf{w}_j - \mathbf{w}_i) + \frac{\Gamma_i}{p_{tx}} (\mathbf{z}_1 - \mathbf{w}_i),$$

containing both the desired disagreement signal, and a distortion term. This distortion contains both a fixed bias term proportional to \mathbf{z}_1 and a signal-dependent drift term proportional to \mathbf{w}_i , which accumulate over time and degrade the convergence performance of DGD.

The primary source of performance degradation is that NCOTA relies on the *energy superposition* property of wireless channels. Specifically, the term “ $-N_0$ ” in (9) compensates for the energy contribution of additive noise. In contrast, in the presence of an unknown interference source, NCOTA inevitably accumulates energy from that interference. If the interference structure is unknown, this accumulated interference energy cannot be compensated for, unlike the noise term “ $-N_0$ ” in (9).

Next, we enhance NCOTA by introducing two key techniques to achieve robustness against interference. We refer to the resulting scheme as *interference-robust* (IR)-NCOTA. We start by decomposing the target disagreement signal in (11) into two components:

$$\mathbf{d}_i = \underbrace{\sum_{j \neq i} \Lambda_{ij} \mathbf{w}_j}_{(a) \triangleq \bar{\mathbf{s}}_i} - \underbrace{\left(\sum_{j \neq i} \Lambda_{ij} \right) \mathbf{w}_i}_{(b) \triangleq \bar{\Lambda}_i}. \quad (12)$$

The first term represents (a) *weighted sum of the local parameter vectors* across the network, weighted by their respective average channel gains. We denote this term as $\bar{\mathbf{s}}_i$ for node i . The second term (b) scales the local parameter vector \mathbf{w}_i (known only to node i) by the *sum of the average channel gains incoming into node i* , denoted as $\bar{\Lambda}_i$. We aim to estimate these two terms separately.

1) *Estimation of the weighted sum of the local parameter vectors, $\bar{\mathbf{s}}_i$:* In the baseline NCOTA algorithm, during the energy encoding process, the local optimization signals are expressed with respect to a fixed and common frame of reference defined by the codewords $\{\mathbf{z}_1, \dots, \mathbf{z}_M\}$, as shown in (5). The resulting vectors \mathbf{p}_i of non-negative coefficients are then used to scale the sample energy of the transmitted signals. This creates a vulnerability, as the transmitted energy becomes

susceptible to interference that accumulates coherently over time with respect to the *fixed* frame of reference.

To estimate \bar{s}_i , we introduce a key mechanism that *scrambles* the distortion caused by the energy of the interference, rendering the interference contribution to the disagreement signal estimation a zero-mean process. To this end, each transmitter applies a *pseudo-random frame-of-reference rotation* to its local parameter vector. This is achieved by applying a coordinated random unitary transformation to each local parameter vector \mathbf{w}_i :

$$\tilde{\mathbf{w}}_i = \mathbf{U} \cdot \mathbf{w}_i,$$

where $\mathbf{U} \in \mathbb{R}^{d \times d}$ satisfies $\mathbf{U}^\top \mathbf{U} = \mathbf{I}$, $\mathbb{E}[\mathbf{U}] = \mathbf{0}$, i.i.d. across iterations, and is common to all nodes in the network (e.g., generated using a pseudo-random sequence with a common seed). An example is a random sign flip $\mathbf{U} = s\mathbf{I}$, where $s \in \{+1, -1\}$ with $\mathbb{P}(s=1) = \mathbb{P}(s=-1) = 1/2$. Importantly, \mathbf{U} is statistically independent of the interference signal \mathbf{n}_i .

Since \mathcal{W} is a sphere centered at $\mathbf{0}$, the rotated vector $\tilde{\mathbf{w}}_i$ also belongs to \mathcal{W} , allowing it to be encoded using the same energy encoding scheme described in Sec. II. Therefore, each transmitting node maps its rotated signal as in (6) to

$$\tilde{\mathbf{p}}_i = \mathcal{P}(\tilde{\mathbf{w}}_i),$$

so that

$$\tilde{\mathbf{w}}_i = \sum_{m=1}^M [\tilde{\mathbf{p}}_i]_m \mathbf{z}_m \Rightarrow \mathbf{w}_i = \sum_{m=1}^M [\tilde{\mathbf{p}}_i]_m \mathbf{U}^\top \mathbf{z}_m. \quad (13)$$

At this point, the nodes follow the same signal encoding in (7) and randomized transmission protocol described in Sec. II, so that node i receives the signal \mathbf{y}_i as in (8). To estimate \bar{s}_i (component (a) in (12)), node i first computes the received sample energy as

$$[\mathbf{r}_i]_m = \chi_i \frac{|\mathbf{y}_i|_m|^2}{(1-p_{tx})p_{tx}EM}, \quad \forall m = 1, \dots, M. \quad (14)$$

Note that $\mathbf{r}_i = \mathbf{0}$ for nodes that operate as transmitters. Compared to the baseline approach in (9), there is no compensation for the noise energy N_0 , since the interference energy contribution is unknown. Finally, node i estimates \bar{s}_i as

$$\hat{s}_i \triangleq \mathbf{U}^\top \sum_{m=1}^M [\mathbf{r}_i]_m \mathbf{z}_m, \quad (15)$$

analogous to the step in (10), followed by a rotation back to the original frame of reference via \mathbf{U}^\top .

Note that, taking the expectation of $[\mathbf{r}_i]_m$, conditional on the frame of reference rotation \mathbf{U} , we obtain

$$\mathbb{E}[[\mathbf{r}_i]_m | \mathbf{U}, \mathbf{w}_j, \forall j] = \sum_{j \neq i} \Lambda_{ij} [\tilde{\mathbf{p}}_j]_m + \frac{\mathbb{E}[\chi_i][\mathbf{n}_i]_m|^2}{(1-p_{tx})p_{tx}EM}, \quad (16)$$

where we used the fact that the interference \mathbf{n}_i is uncorrelated with the fading channels h_{ij} , and the independence of χ_i and \mathbf{n}_i from \mathbf{U} . It then follows

$$\mathbb{E}[\hat{s}_i | \mathbf{U}, \mathbf{w}_j, \forall j] = \sum_{j \neq i} \Lambda_{ij} \mathbf{w}_j + \sum_{m=1}^M \frac{\mathbb{E}[\chi_i][\mathbf{n}_i]_m|^2}{(1-p_{tx})p_{tx}EM} \mathbf{U}^\top \mathbf{z}_m,$$

after replacing (16) into (15), since χ_i , \mathbf{n}_i are statistically independent of \mathbf{U} . Finally, taking expectation with respect to \mathbf{U} , and using $\mathbb{E}[\mathbf{U}] = \mathbf{0}$, we obtain

$$\mathbb{E}[\hat{s}_i | \mathbf{w}_j, \forall j] = \sum_{j \neq i} \Lambda_{ij} \mathbf{w}_j, \quad (17)$$

so that \hat{s}_i is an unbiased estimate of \bar{s}_i .

2) *Estimation of the sum of the average channel gains*, $\bar{\Lambda}_i$: Next, we address the estimation of the sum channel gains $\bar{\Lambda}_i$. To this end, each transmitting node sends a pseudo-random pilot sequence $\mathbf{x}_P \in \mathbb{C}^{n_P}$ of length $n_P \geq 2$, defined as $[\mathbf{x}_P]_m = \sqrt{E} e^{j\phi_m}$, where $\phi_m \sim \mathcal{U}([0, 2\pi])$ are random phases, i.i.d. over m and across time, but common across the network and independent of the interference signal. Note that $\mathbb{E}[\mathbf{x}_P] = \mathbf{0}$ and $\mathbb{E}[\mathbf{x}_P \cdot \mathbf{x}_P^\top] = E\mathbf{I}$.

The received pilot observation at node i is

$$\mathbf{y}_{P,i} = \sum_{j: \chi_j=0} h_{ij} \mathbf{x}_P + \mathbf{n}_{P,i},$$

where $\mathbf{n}_{P,i}$ denotes the interference signal during pilot transmission. Upon receiving $\mathbf{y}_{P,i}$, node i estimates $\bar{\Lambda}_i$ as

$$\begin{aligned} \hat{\Lambda}_i &= \frac{\chi_i}{(1-p_{tx})p_{tx}En_P(n_P-1)} \left[\frac{1}{E} |\mathbf{x}_P^\top \mathbf{y}_{P,i}|^2 - \|\mathbf{y}_{P,i}\|^2 \right] \\ &= \frac{\chi_i}{(1-p_{tx})p_{tx}En_P(n_P-1)} \sum_{m,n=1: m \neq n}^{n_P} e^{j(\phi_n - \phi_m)} [\mathbf{y}_{P,i}]_m [\mathbf{y}_{P,i}]_n^*. \end{aligned}$$

Note that $\hat{\Lambda}_i = 0$ for nodes operating as transmitters.

To compute the expectation of this estimate, consider

$$\begin{aligned} e^{j(\phi_n - \phi_m)} [\mathbf{y}_{P,i}]_m [\mathbf{y}_{P,i}]_n^* &= E \left| \sum_{j: \chi_j=0} h_{ij} \right|^2 \\ &\quad + e^{j(\phi_n - \phi_m)} [\mathbf{n}_{P,i}]_m [\mathbf{n}_{P,i}]_n^* \\ &\quad + \sqrt{E} \sum_{j: \chi_j=0} (h_{ij}^* e^{-j\phi_m} [\mathbf{n}_{P,i}]_m + h_{ij} e^{j\phi_n} [\mathbf{n}_{P,i}]_n^*). \end{aligned}$$

Taking the expectation with respect to the pseudo-random pilot phases and using the facts that $\mathbb{E}[e^{j\phi_n}] = 0$, $\mathbb{E}[e^{j(\phi_n - \phi_m)}] = 0$ for $n \neq m$, and that the interference signal is independent of the pilot phases, we obtain for $n \neq m$

$$\begin{aligned} \mathbb{E}[e^{j(\phi_n - \phi_m)} [\mathbf{y}_{P,i}]_m [\mathbf{y}_{P,i}]_n^*] &= E \cdot \mathbb{E} \left[\left| \sum_{j: \chi_j=0} h_{ij} \right|^2 \right] \\ &= E p_{tx} \sum_{j \neq i} \Lambda_{ij}, \end{aligned}$$

where the last equality follows by taking the expectation with respect to the random transmission decisions and the Rayleigh fading coefficients. Hence, it follows that

$$\mathbb{E}[\hat{\Lambda}_i] = \frac{1}{n_P(n_P-1)} \sum_{m,n=1}^{n_P} \sum_{j \neq i, m \neq n} \Lambda_{ij} = \sum_{j \neq i} \Lambda_{ij} = \bar{\Lambda}_i, \quad (18)$$

so that $\hat{\Lambda}_i$ is an unbiased estimate of the sum of channel gains $\bar{\Lambda}_i$.

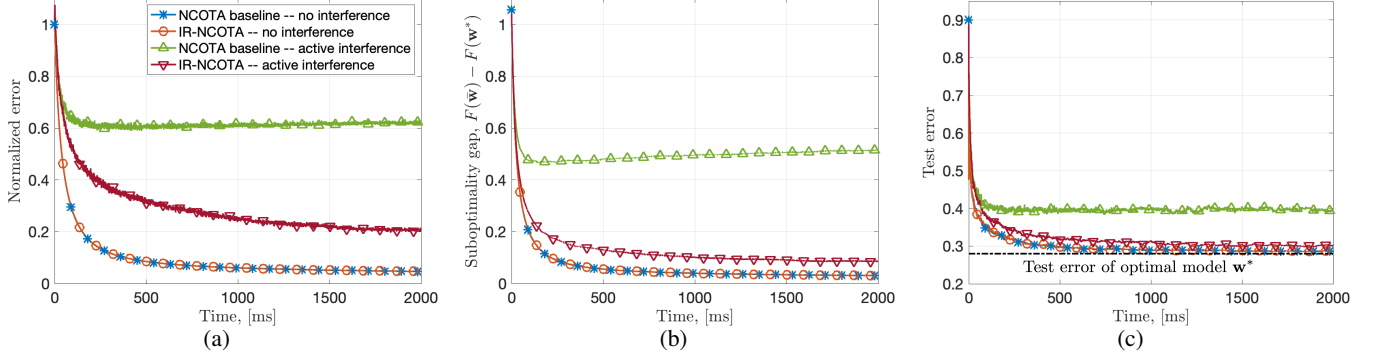


Fig. 2: Normalized error (a), suboptimality gap (b), and test error (c), vs execution time. Common legend shown in figure (a).

Finally, node i combines the two estimates to estimate the disagreement signal as

$$\hat{\mathbf{d}}_i = \hat{\mathbf{s}}_i - \hat{\Lambda}_i \mathbf{w}_i = \mathbf{U}^\top \sum_{m=1}^M [\mathbf{r}_i]_m \mathbf{z}_m - \hat{\Lambda}_i \mathbf{w}_i. \quad (19)$$

Using (17) and (18), it follows directly that $\hat{\mathbf{d}}_i$ is an unbiased estimate of the disagreement signal \mathbf{d}_i , and hence the convergence properties established in [19] remain valid.

In the next section, we present numerical results demonstrating the performance gains of IR-NCOTA over the baseline NCOTA algorithm in the presence of interference.

IV. NUMERICAL RESULTS

We evaluate the performance of the proposed IR-NCOTA algorithm on a classification task using the Fashion-MNIST dataset [23], which contains grayscale images of fashion products from 10 classes.

Network deployment: $N = 200$ nodes are uniformly and independently distributed over a circular area with a radius of 2 km. The nodes communicate over a total bandwidth of $W_{\text{tot}} = 5$ MHz at a carrier frequency of $f_c = 3$ GHz, with transmit power $P_{\text{tx}} = 20$ dBm. The receiver noise power spectral density is $N_0 = -173$ dBm/Hz.

Channel model: Channels are modeled as Rayleigh fading, $h_{ij} \sim \mathcal{CN}(0, \Lambda_{ij})$, independently across node pairs and DGD iterations. The average channel gain Λ_{ij} follows Friis' free-space path-loss model, i.e.,

$$\Lambda_{ij} = \left(\frac{\lambda}{4\pi d_{ij}} \right)^2,$$

where λ is the signal wavelength and d_{ij} is the distance between nodes i and j .

Data deployment: Each node stores a local dataset of five low-resolution images belonging to a single class. Thus, 20 nodes hold data with label '0', 20 with label '1', and so on. Let $\ell_i \in \{0, \dots, 9\}$ denote the label associated with node i . Each 7×7 pixel image is transformed into a 50-dimensional feature vector $\mathbf{f} \in \mathbb{R}^{50}$ (including a bias term) and normalized such that $\|\mathbf{f}\| = 1$.

Optimization problem: The learning task is formulated as a regularized logistic regression problem with loss function

$$\phi(\ell, \mathbf{f}; \mathbf{w}) = \frac{\mu}{2} \|\mathbf{w}\|^2 - \ln \left(\frac{\exp\{\mathbf{f}^\top \mathbf{w}^{(\ell)}\}}{\sum_{j=0}^9 \exp\{\mathbf{f}^\top \mathbf{w}^{(j)}\}} \right),$$

where $\mathbf{w}^\top = [\mathbf{w}^{(1)\top}, \dots, \mathbf{w}^{(9)\top}] \in \mathbb{R}^d$ with $d = 450$, $\mathbf{w}^{(\ell)} \in \mathbb{R}^{50}$, $\mathbf{w}^{(0)} = \mathbf{0}$, and $\mu = 0.001$. The local objective function at node i is defined as

$$f_i(\mathbf{w}) = \frac{1}{|\mathcal{D}_i|} \sum_{\mathbf{f} \in \mathcal{D}_i} \phi(\ell_i, \mathbf{f}; \mathbf{w}).$$

The functions $f_i(\mathbf{w})$, and consequently the global objective $F(\mathbf{w})$, are strongly convex with parameter $\mu = 0.001$ and smooth with parameter $L = \mu + 2$.

Algorithms: We compare the baseline NCOTA algorithm from [19] with the proposed interference-robust (IR-NCOTA) scheme under two settings:

- **No interference:** in this case, there is only additive noise $\mathbf{n}_i \sim \mathcal{CN}(\mathbf{0}, N_0 \mathbf{I})$.
- **Active interference:** An interference source located at the center of the deployment area emits a Gaussian signal $\mathbf{v} \sim \mathcal{CN}(\mathbf{0}, EI)$, where $E = P_{\text{tx}}/W_{\text{tot}}$ is the transmitted signal energy. This is received through a Rayleigh fading channel $g_i \sim \mathcal{CN}(\mathbf{0}, \Gamma_i)$, where Γ_i is the average channel gain between the interferer and node i , following Friis' model. In this case, the total interference-plus-noise at node i is $\mathbf{n}_i = g_i \mathbf{v} + \mathcal{CN}(\mathbf{0}, N_0 \mathbf{I})$.

For the baseline NCOTA, $M = 2d + 1$ samples are transmitted per iteration, yielding a time-frame duration of $M/W_{\text{tot}} = 180.2\mu\text{s}$. For IR-NCOTA, we generate the random unitary transformation as $\mathbf{U} = s\mathbf{I}$ (sign flip), where $s = \pm 1$ with $\mathbb{P}(s=1) = \mathbb{P}(s=-1) = 1/2$, and use a pilot sequence of length $n_P = 10$, corresponding to a modest pilot overhead of $\approx 1\%$, and a time-frame duration of $(M+n_P)/W_{\text{tot}} = 182.2\mu\text{s}$. The transmission probability is set to $p_{tx} = 0.34$.

Algorithm parameters: Both algorithms use decreasing step-size sequences²

$$\gamma_k = \frac{\gamma_0}{(1+k\delta)^{3/4}}, \quad \eta_k = \frac{\eta_0}{(1+k\delta)},$$

for the consensus and learning steps, respectively, at DGD iteration k . Following the theoretical convergence analysis in [19], the initial parameters are set as $\gamma_0 = 1.7 \times 10^7$, $\eta_0 = 2/(\mu+L)$, and $\delta = \frac{5}{4\mu\eta_0}$. Both schemes are initialized as $\mathbf{w}_i = \mathbf{0}, \forall i$. The optimization set \mathcal{W} has radius $r = \|\nabla F(\mathbf{0})\|/\mu$.

Evaluations and Discussion: We evaluate the following performance metrics vs running time: (a) the normalized

²We refer the interested reader to the convergence proof in [19] for a detailed justification of these parameter choices.

error $\frac{1}{N} \sum_{i=1}^N \|\mathbf{w}_i - \mathbf{w}^*\|^2 / \|\mathbf{w}^*\|^2$, measuring the deviation of the local models from the global optimum in (1); (b) the *suboptimality gap* $F(\bar{\mathbf{w}}) - F(\mathbf{w}^*)$ of the average model across the network, $\bar{\mathbf{w}} = \frac{1}{N} \sum_i \mathbf{w}_i$; and (c) the *test error*, $\text{TEST}(\bar{\mathbf{w}})$, of the averaged model, computed on a test set of 1000 samples (100 per class), with the predicted label for a feature vector \mathbf{f} given by $\arg \max_{\ell} \mathbf{w}^{(\ell)\top} \mathbf{f}$.

All results are averaged over 20 independent realizations of the network topology, noise, interference, transmission decisions, and—specifically for IR-NCOTA—the pseudo-random sign flips and pilot phases, as described in Secs. II and III.

The results are depicted in Fig. 2. When the interference is inactive, IR-NCOTA performs comparably to the baseline NCOTA algorithm across all metrics. All error measures exhibit a decreasing trend, with the suboptimality gap approaching zero and the test error converging to that obtained under the global optimum \mathbf{w}^* . It is worth noting that the baseline NCOTA algorithm exploits knowledge of the noise variance N_0 to compensate for the accumulation of noise energy, whereas the interference-robust scheme operates without such information. Nonetheless, there is no appreciable loss in performance due to the lack of knowledge of N_0 .

When the interference is active, however, the baseline NCOTA algorithm fails to converge: all metrics reach a floor, indicating a persistent gap from the optimal solution. This behavior results from the accumulation of interference energy, which induces a drift in the learned model. In contrast, IR-NCOTA successfully mitigates this effect by making the interference contribution appear as a zero-mean process. By eliminating the drift, the error metrics under IR-NCOTA continue to decrease, although at a slower rate compared to the interference-free case due to the higher variance in the disagreement signal estimates. Overall, these results demonstrate the robustness of the proposed IR-NCOTA scheme against external interference sources.

V. CONCLUSIONS

This paper presented a novel *Interference-Robust Non-Coherent Over-the-Air* (IR-NCOTA) computation scheme for decentralized optimization over wireless networks. Building upon the NCOTA framework, which enables decentralized consensus without channel state information or transmission scheduling, the proposed IR-NCOTA extends its applicability to environments affected by external interference. The core contribution lies in introducing two complementary mechanisms: a coordinated random rotation of the frame of reference and a pseudo-random pilot transmission, that jointly render the distortion introduced by the interfering signal zero-mean in expectation. This preserves the unbiasedness of the disagreement signal estimates and, consequently, the convergence guarantees of DGD. Numerical evaluations confirm that IR-NCOTA achieves comparable performance to baseline NCOTA in interference-free conditions and maintains convergence under external interference, where conventional NCOTA fails.

REFERENCES

- [1] S. Kar and J. M. Moura, “Consensus + innovations distributed inference over networks: cooperation and sensing in networked systems,” *IEEE Signal Processing Magazine*, vol. 30, no. 3, pp. 99–109, 2013.
- [2] T. T. Doan, S. T. Maguluri, and J. Romberg, “Convergence Rates of Distributed Gradient Methods Under Random Quantization: A Stochastic Approximation Approach,” *IEEE Transactions on Automatic Control*, vol. 66, no. 10, pp. 4469–4484, 2021.
- [3] A. Nedić, J.-S. Pang, G. Scutari, and Y. Sun, *Multi-agent Optimization*, 1st ed. Springer, Cham, 2018.
- [4] T. Yang, X. Yi, J. Wu, Y. Yuan, D. Wu, Z. Meng, Y. Hong, H. Wang, Z. Lin, and K. H. Johansson, “A survey of distributed optimization,” *Annual Reviews in Control*, vol. 47, pp. 278–305, 2019.
- [5] A. Khan, S. Gupta, and S. K. Gupta, “Emerging uav technology for disaster detection, mitigation, response, and preparedness,” *Journal of Field Robotics*, vol. 39, no. 6, pp. 905–955, 2022.
- [6] Y. Xiao, Y. Ye, S. Huang, L. Hao, Z. Ma, M. Xiao, S. Mumtaz, and O. A. Dobre, “Fully Decentralized Federated Learning-Based On-Board Mission for UAV Swarm System,” *IEEE Communications Letters*, vol. 25, no. 10, pp. 3296–3300, 2021.
- [7] S. Savazzi, M. Nicoli, and V. Rampa, “Federated learning with cooperating devices: A consensus approach for massive iot networks,” *IEEE Internet of Things Journal*, vol. 7, no. 5, pp. 4641–4654, 2020.
- [8] A. Nedic and A. Ozdaglar, “Distributed subgradient methods for multi-agent optimization,” *IEEE Transactions on Automatic Control*, vol. 54, no. 1, pp. 48–61, 2009.
- [9] K. Yuan, Q. Ling, and W. Yin, “On the Convergence of Decentralized Gradient Descent,” *SIAM Journal on Optimization*, vol. 26, no. 3, pp. 1835–1854, 2016.
- [10] N. Michelusi, “CSI-Free Over-The-Air Decentralized Learning Over Frequency Selective Channels,” in *IEEE International Conference on Acoustics, Speech and Signal Processing (ICASSP)*, 2024, pp. 13076–13080.
- [11] ———, “Decentralized Federated Learning via Non-Coherent Over-the-Air Consensus,” in *ICC 2023 - IEEE International Conference on Communications*, 2023, pp. 3102–3107.
- [12] H. Xing, O. Simeone, and S. Bi, “Federated Learning Over Wireless Device-to-Device Networks: Algorithms and Convergence Analysis,” *IEEE Journal on Selected Areas in Communications*, vol. 39, no. 12, pp. 3723–3741, 2021.
- [13] Y. Shi, Y. Zhou, and Y. Shi, “Over-the-Air Decentralized Federated Learning,” in *2021 IEEE International Symposium on Information Theory (ISIT)*, 2021, pp. 455–460.
- [14] E. Ozfatura, S. Rini, and D. Gündüz, “Decentralized SGD with Over-the-Air Computation,” in *IEEE GLOBECOM 2020*, 2020, pp. 1–6.
- [15] Z. Jiang, G. Yu, Y. Cai, and Y. Jiang, “Decentralized Edge Learning via Unreliable Device-to-Device Communications,” *IEEE Transactions on Wireless Communications*, vol. 21, no. 11, pp. 9041–9055, 2022.
- [16] H. Ye, L. Liang, and G. Y. Li, “Decentralized Federated Learning With Unreliable Communications,” *IEEE Journal of Selected Topics in Signal Processing*, vol. 16, no. 3, pp. 487–500, 2022.
- [17] E. Jeong, M. Zecchin, and M. Kountouris, “Asynchronous Decentralized Learning over Unreliable Wireless Networks,” in *ICC 2022 - IEEE International Conference on Communications*, 2022, pp. 607–612.
- [18] E. G. Larsson and N. Michelusi, “Unified Analysis of Decentralized Gradient Descent: A Contraction Mapping Framework,” *IEEE Open Journal of Signal Processing*, vol. 6, pp. 507–529, 2025.
- [19] N. Michelusi, “Non-coherent over-the-air decentralized gradient descent,” *IEEE Transactions on Signal Processing*, vol. 72, pp. 4618–4634, 2024.
- [20] A. Reisizadeh, A. Mokhtari, H. Hassani, and R. Pedarsani, “An exact quantized decentralized gradient descent algorithm,” *IEEE Transactions on Signal Processing*, vol. 67, no. 19, pp. 4934–4947, 2019.
- [21] G. Zhu, Y. Wang, and K. Huang, “Broadband analog aggregation for low-latency federated edge learning,” *IEEE Transactions on Wireless Communications*, vol. 19, no. 1, pp. 491–506, 2020.
- [22] A. Ogierman, A. Richa, C. Scheideler, S. Schmid, and J. Zhang, “Competitive mac under adversarial sinr,” in *IEEE INFOCOM 2014 - IEEE Conference on Computer Communications*, 2014, pp. 2751–2759.
- [23] H. Xiao, K. Rasul, and R. Vollgraf, “Fashion-mnist: a novel image dataset for benchmarking machine learning algorithms,” *CoRR*, vol. abs/1708.07747, 2017.